

ATR-FTIR Spectroscopy Study of the Influence of pH and Contact Time on the Adhesion of *Shewanella putrefaciens* Bacterial Cells to the Surface of Hematite

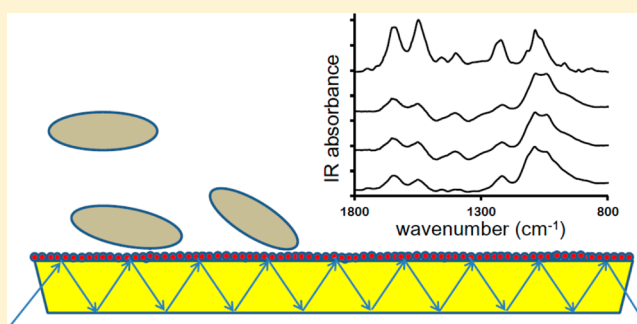
Evert J. Elzinga,^{†,*} Jen-How Huang,[‡] Jon Chorover,[§] and Ruben Kretschmar[‡]

[†]Department of Earth & Environmental Sciences, Rutgers University, Newark, New Jersey, United States

[‡]Institute of Biogeochemistry and Pollutant Dynamics, ETH Zurich, Zurich, Switzerland

[§]Department of Soil, Water and Environmental Science, University of Arizona, Tucson, Arizona, United States

ABSTRACT: Attachment of live cells of *Shewanella putrefaciens* strain CN-32 to the surface of hematite ($\alpha\text{-Fe}_2\text{O}_3$) was studied with in situ ATR-FTIR spectroscopy at variable pH (4.5–7.7) and contact times up to 24 h. The IR spectra indicate that phosphate based functional groups on the cell wall play an important role in mediating adhesion through formation of inner-sphere coordinative bonds to hematite surface sites. The inner-sphere attachment mode of microbial P groups varies with pH, involving either a change in protonation or in coordination to hematite surface sites as pH is modified. At all pH values, spectra collected during the early stages of adhesion show intense IR bands associated with reactive P-groups, suggestive of preferential coordination of P-moieties at the hematite surface. Spectra collected after longer sorption times show distinct frequencies from cell wall protein and carboxyl groups, indicating that bacterial adhesion occurring over longer time scales is to a lesser degree associated with preferential attachment of P-based bacterial functional groups to the hematite surface. The results of this study demonstrate that pH and reaction time influence cell-mineral interactions, implying that these parameters play an important role in determining cell mobility and biofilm formation in aqueous geochemical environments.



INTRODUCTION

The attachment of bacterial cells to mineral surfaces is a process relevant to a broad variety of disciplines including geochemistry, microbiology, drinking water engineering, petroleum exploration, and medical biology.^{1–10} Adhesion of microbial cells is a critical step in the formation of biofilms, which play an important role in the biogeochemistry of aqueous geochemical environments through processing of nutrients and organic matter, and adsorption of trace elements and pollutants.^{11–13} Bacterial cell attachment to mineral surfaces influences other major geochemical processes as well, including reductive dissolution of Mn(III, IV)- and Fe(III)-oxides, which may require close contact between the microbial cell and the oxide surface to facilitate electron flow, and mineral weathering, which may be promoted by microbial metabolites produced at the mineral surface.^{7,14–17} Recent work has shown that microbial attachment to mineral surfaces may enhance trace metal(loid) solubility in aqueous environments by mobilizing sorbed impurities from surface sites through competitive displacement by reactive functional groups on the microbial cell wall.^{18–20}

The processes involved in the initial attachment of suspended microbial cells to mineral surfaces are not completely understood. Bacterial cell walls are composed of

teichoic acids (in the case of Gram-positive bacteria), lipopolysaccharides (Gram-negative bacteria), surface proteins, and extracellular polymeric substances (EPS), which are a heterogeneous mixture of polysaccharides, proteins, nucleic acid, and lipids.^{21–23} Major reactive groups found on the cell wall surface are carboxyl and phosphate moieties, which have been identified as active sites in removing dissolved metal cations from solution through inner-sphere complexation, as well as in mediating cell attachment to mineral substrates through the formation of covalent bonds.^{24–31} The various functional groups exhibit pH dependent protonation/deprotonation reactions, which render bacterial cells negatively charged at typical environmental pH values,^{32,33} thereby facilitating electrostatically favorable interactions between bacteria and the surfaces of common Fe(III)-(oxyhydr)oxides, which are positively charged over most of the environmental pH range.³⁴ The overall process of microbial adhesion involves a complex interplay of long-range Coulombic and van der Waals interactions in combination with short-range chemical inter-

Received: August 15, 2012

Revised: October 28, 2012

Accepted: November 8, 2012

Published: November 8, 2012

actions between biomolecules on microbial cell walls and the surface.^{35–40}

The current contribution focuses on the adhesion of *Shewanella putrefaciens* bacterial cells to the surface of hematite ($\alpha\text{-Fe}_2\text{O}_3$) as studied by ATR-FTIR spectroscopy. *Shewanella putrefaciens* is a Gram-negative, facultative anaerobe, capable of dissimilatory reduction of Fe(III)-oxides in natural environments.⁴⁰ ATR-FTIR spectroscopy has been successfully applied in previous studies dealing with the characterization of microbial cells and their attachment to Fe(III)-oxide surfaces.^{18,28,30,31,37,41–45} These studies have pointed to the importance of organic phosphate and carboxylate groups in mediating cell adhesion to Fe(III)-oxides, reporting formation of inner-sphere covalent bonds between these reactive moieties and surface Fe atoms during adhesion of Gram-positive and Gram-negative bacterial cells and EPS biomolecules.^{30,31,41–45} Inner-sphere coordination of orthophosphate, phosphonates and carboxylates onto iron oxides varies mechanistically with pH.^{46–51} Therefore, pH is also likely to affect the molecular level processes involved in the interaction between microbial cell walls and Fe(III)-oxides surfaces, but this has not been addressed in previous spectroscopic studies. The effect of time is of interest as well, since substantial conformational and chemical changes may occur during the early stages of microbial cell contact with Fe(III)-oxide mineral particles.³⁷ The aim of the current study was to use ATR-FTIR spectroscopy to assess the main functional group(s) involved in the interaction between *S. putrefaciens* cells and the hematite surface, and to investigate mechanistic changes in the reactions involved as a function of pH and reaction time.

MATERIALS AND METHODS

Hematite Preparation. The hematite sorbent used for the experiments was synthesized based on a procedure described by Sugimoto et al.⁵² Briefly, 500 mL of a 2 M FeCl_3 solution was slowly added over the course of 5 min to 500 mL of a propeller-stirred 5.4 M NaOH solution. The resulting gel was aged in a sealed Pyrex glass bottle at 101 °C for 8 days. After cooling to room temperature, the product was repeatedly washed with doubly deionized (DDI) water (18.2 M Ω cm, Milli-Q, Millipore) until the electrical conductivity was $<5 \mu\text{S cm}^{-1}$, and then freeze-dried. X-ray diffraction analysis confirmed the material was hematite and showed no evidence for the presence of other crystalline phases. The N_2 -BET specific surface area of the hematite was 24 m² g⁻¹, and the point of zero charge was 9.3 as determined from the common intersection point of acid–base titrations at different ionic strengths. A more detailed characterization can be found in the Supporting Information of Brechbühl et al.⁵³

***Shewanella putrefaciens* Preparation.** *Shewanella putrefaciens* strain CN-32 was obtained from the AAS as ATCC BAA-1097. For each experiment, the bacteria were grown under aerobic conditions to late exponential growth in a 1 L volume of Tryptone/Fluka growth medium held in a bottle with a 100 mL headspace and capped loosely to allow gas exchange. The bottle was placed on an orbital shaker operating at 100 rpm, and growth was allowed to proceed for 24 h at 30 °C. The resulting bacterial suspension had an optical density measured with UV-vis at 600 nm (OD_{600}) of 0.20, and was distributed over 50 mL tubes which were centrifuged at 2100g for 15 min at 4 °C to harvest the cells. The supernatants were discarded, and the remaining bacterial pellets were washed repeatedly by resuspending the bacteria in 0.1 M NaCl at pH 7.0 followed by

centrifugation (2100g, 15 min at 4 °C). After the third wash, the bacterial pellets were combined in a single tube, and an appropriate volume of 0.1 M NaCl was added to obtain a bacterial stock suspension with a cell density of 10^{10} cells mL⁻¹ as determined from OD_{600} measurements calibrated against total cell numbers determined by counting of DAPI (4',6-diamidino-2-phenylindol)-stained cells using an optical microscope (Leica Microsystems, Wetzlar, Germany).

ATR-FTIR Experiments. The ATR-FTIR spectra were recorded on a Perkin-Elmer Spectrum One spectrometer equipped with a purge gas generator and a liquid N₂-cooled MCT-A detector. Adhesion experiments employed an ATR-FTIR flow-cell setup similar to those described in other studies.^{18,46,54} A horizontal 45° ZnSe ATR crystal was coated with a hematite film (≈ 1.0 mg) by drying 200 μL of a finely dispersed 5 g L⁻¹ hematite suspension evenly spread across the crystal surface, which produced a stable deposit firmly adhered to the ZnSe crystal. The coated crystal was sealed in a flow cell, placed on the ATR stage inside the IR spectrometer, and connected to a reaction vessel containing 500 mL of 0.1 M NaCl electrolyte adjusted to the desired pH. A peristaltic pump was used to circulate solute from the reaction vessel through the flow cell at a rate of 2 mL min⁻¹. The pH of the solution in the main reaction vessel was monitored throughout the experiment and readjusted as necessary. The hematite deposit was equilibrated with the background solution for approximately 4 h. A background spectrum consisting of the combined absorbances of the ZnSe crystal, the hematite deposit and the reaction electrolyte was then collected as the average of 250 coadded scans at a 4 cm⁻¹ resolution, and all successive spectra were ratioed to this background spectrum.

Shewanella putrefaciens cell adhesion to hematite was studied in the pH range 4.5–7.7, at reaction times up to 24 h. The adhesion experiments were performed in the absence of organic substrates to maintain constant biomass and prevent production of metabolites. Adhesion experiments were conducted at constant pH (4.5, 6.4, or 7.7) and were started by injecting a 0.5 mL aliquot of the bacterial stock suspension into the main reaction vessel to achieve a cell density of 10^7 cells mL⁻¹. Cell adhesion to the hematite deposit was monitored by observing characteristic absorbances of bacterial functional groups in the 1600–700 cm⁻¹ spectral range. Attachment was allowed to proceed for 24 h with data collected every few hours to monitor the adhesion process over time. At the end of the experiment, the hematite deposit on the ZnSe crystal was checked for any signs of film erosion, which were not observed. Previous studies employing atomic force and electrostatic force microscopy (AFM and EFM) and scanning electron microscopy (SEM) to characterize of *Shewanella putrefaciens* microbial cells following contact with solutions of variable pH have indicated that solution pH (in the range 2.5–10) affects the charge and mechanical properties of the cell surface, but report no evidence for cell lysis.^{33,55–57} Garioud et al.⁵⁷ concluded based on total cell counts of *Shewanella putrefaciens* cells incubated at pH 4.0 and pH 10.0 that no significant cell lysis occurred. Based on these studies and given the relatively mild pH conditions of the experiments conducted here (pH 4.5–7.7) we assume that cells were intact during the adhesion experiments.

To assist and constrain interpretation of the bacterial adhesion data, a set of ATR-FTIR reference spectra was collected as well. Spectra of aqueous bacterial suspensions were obtained by taking scans of 10^9 cells mL⁻¹ suspensions, from

which the ZnSe and H₂O absorbances were subtracted to isolate the contributions from the microbial cells.¹⁸ Spectra of aqueous and adsorbed complexes of adenosine 5'-monophosphate (AMP), and *N,N,N*-trimethyl-2-(phosphonoxy)-ethanaminium (phosphocholine) were collected as well. Both AMP and phosphocholine are organic compounds with terminal phosphate groups, which have been implicated in mediating adhesion between bacterial EPS and mineral surfaces.³⁷ For further reference, spectra were also collected for orthophosphate complexes adsorbed on hematite. Sorption experiments with AMP, phosphocholine, and orthophosphate were performed with the same flow cell setup and experimental techniques described above for the bacterial adhesion studies, using aqueous reactant concentration of 50 μM, and pH values in the range 4.5–6.5. Spectra of dissolved AMP, orthophosphate and phosphocholine were collected by scanning solutions containing 0.1 M of the compound of interest adjusted to the desired pH, followed by subtraction of ZnSe and H₂O absorbances.

The thickness of the hematite deposit used in the flow cell experiments was estimated at 0.7 μm, based on the amount of hematite on the ATR cell (1.0 mg), the dimension of the ZnSe ATR cell surface (7 cm²), and an estimated density of 2 g cm⁻³ for the hydrated hematite deposit.⁵⁴ For a 45° ZnSe ATR crystal such as used here, the penetration depth of IR light in water is 1.39 μm at 1100 cm⁻¹.^{54,58} Given that the hematite layer has a refractive index higher than that of H₂O,^{54,59} the IR beam probes the entire thickness of the hematite deposit and protrudes into the aqueous phase overlying the hematite film. *S. putrefaciens* bacterial cells cultivated under the conditions employed here are tubular with a length of 2–3 μm, and a cell wall thickness of ~50 nm.^{60,61} The IR evanescent wave is expected to penetrate the interior of bacterial cells adhered to hematite particles in the flow experiments, and of cells in direct contact with the ZnSe crystal in the experiments characterizing aqueous bacterial suspensions. Estimates of actual penetration depths into cells are, however, problematic due to uncertainty in the refractive indices of bacterial cell walls, and due to variable thickness of the water layer between bacterial cells and the ZnSe crystal and hematite surfaces.⁴²

RESULTS AND DISCUSSION

Figure 1 presents the ATR-FTIR spectra of *S. putrefaciens* cells, collected using a bare (i.e., nonhematite coated) ZnSe ATR crystal in contact with bacterial suspensions with a density of 10⁹ cells mL⁻¹ adjusted to the desired pH. In analogy to IR studies of inorganic species, we refer to these as spectra of “aqueous” bacterial cells; however, it should be noted that the negative charge of the ZnSe ATR crystal surface may affect the IR spectrum of suspended bacterial cells (which contain negatively charged functional groups) in the near surface region probed by the IR beam through electrostatic effects.³⁷ The spectra shown in Figure 1 are consistent with previous ATR-FTIR studies characterizing bacterial cells in aqueous suspension,^{18,31,37,42,43} and illustrate the range of bacterial functional groups accessible to ATR-FTIR characterization in the mid-IR range (400–4000 cm⁻¹). The main peaks and their assignments are summarized in Table 1. The intense peaks at ~1650 and 1550 cm⁻¹ represent the amide I and amide II vibrations of cell proteins, whereas the bands between 1150 and 950 cm⁻¹ are a complex composite of various overlapping P–O, C–O, C–O–C, and C–O–P stretching vibrations associated with phosphoryl groups and polysaccharides

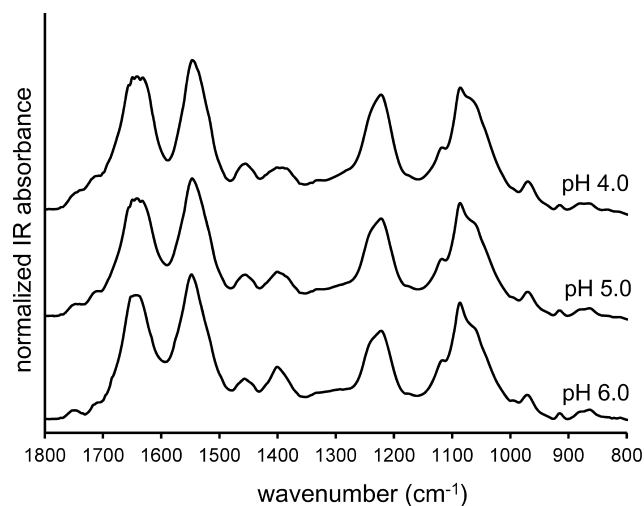


Figure 1. ATR-FTIR spectra of aqueous *S. putrefaciens* suspensions at different pH values. Spectra were collected for suspensions with a cell density of 10⁹ cells mL⁻¹ using a horizontal 45° ZnSe ATR crystal. Assignments of the IR bands are presented in Table 1.

Table 1. Identification of Absorption Bands in the Mid-IR Spectra of *S. putrefaciens* Cells, Adapted from Assignments Provided in References 37, 42, and 43

wavenumber (cm ⁻¹)	IR band assignment
1720–1729	C=O stretch in COOH
1652–1637	amide I: C=O stretching, –CN and –NH bending in amines
1550–1540	amide II: N–H bending, C–N stretching
1454–1482	bending of CH ₂ /CH ₃
1360–1450	$\nu_{as}(\text{COO}^-)$
1210–1270	$\nu(\text{C–OH})$ in COOH; P=O stretch in phosphates
1150–950	asymmetric and symmetric stretching of phosphate PO ₂ and P(OH) ₂
1114–1118	$\nu(\text{C–O–P}, \text{P–O–P})$, ring vibrations
1084–1094	$\nu_s(\text{PO}_2)$; ring vibrations; $\nu(\text{C–O})$; P=O stretch in phosphodiester, phosphorylated proteins, and polyphosphates
1048–1078	C–OH, C–O–C, and C–C vibrations of polysaccharides
1039–1043	$\nu(\text{P–OH}, \text{P–OFe})$
1016–1020	$\nu(\text{P–OFe})$, ring vibrations
962–979	fully symmetric (ν_1) stretching of PO ₃ and PO ₂

(Table 1), making specific band assignments difficult. Bands seen between 1200 and 1250 cm⁻¹ are consistent with P=O stretching in phosphoryl groups and phosphodiester and with C–OH vibrations of protonated carboxyl groups^{42,43} (Table 1). Bands at 1400 and 1730 cm⁻¹ represent the asymmetric C–O stretching bands of deprotonated carboxyl groups ($\nu_{as}(\text{COO}^-)$), and the carbonyl stretch ($\nu(\text{C=O})$) of protonated carboxyl groups, respectively, whereas the band at 1450 cm⁻¹ is assigned to bending vibrations of CH₂/CH₃ (Table 1). The symmetric C–O stretching bands of non-protonated carboxyl groups ($\nu_s(\text{COO}^-)$) occur near 1600 cm⁻¹ where they are obscured by the intense amide I vibrations.^{37,43,49,50} The results presented in Figure 1 demonstrate that absorbance in the mid-IR range effectively detects microbial carboxyl and phosphoryl groups, which have been implicated in mediating bacterial cell interactions with mineral surfaces and with aqueous metal species.^{24–31}

The spectra collected at different pH show clear differences (Figure 1) consistent with proton/deprotonation reactions of functional groups in the pH range of 4.0 to 6.0 considered here. Distinct changes are observed for the carboxyl groups, with lower pH values leading to an increase in the intensity of carbonyl stretching ($1750\text{--}1700\text{ cm}^{-1}$) concurrent with decreasing intensity of the asymmetric stretching band of deprotonated carboxyl units ($\sim 1400\text{ cm}^{-1}$) as carboxyl groups become protonated. Slight changes observed in the amide bands (~ 1650 and $\sim 1550\text{ cm}^{-1}$) may be due to changes in the intensity of symmetric C–O stretching of deprotonated carboxyl (near 1600 cm^{-1} ; obscured by the amide bands) with pH, but may additionally reflect conformational changes of surface proteins.⁴² Changes with pH are also observed in the region containing the various P–O, C–O–C, and C–O–P vibrational modes ($1150\text{--}900\text{ cm}^{-1}$); however, spectral band overlap in this region complicates identification of the specific functional moieties involved. The response to solution pH observed for the spectra in Figure 1 demonstrates that a substantial fraction of the microbial functional groups probed is susceptible to proton exchange with solution, and may thus be available for interaction with other aqueous species as well.

To assess cell-hematite interactions, Figure 2 compares the ATR-FTIR spectra of bacterial cells adhered to hematite

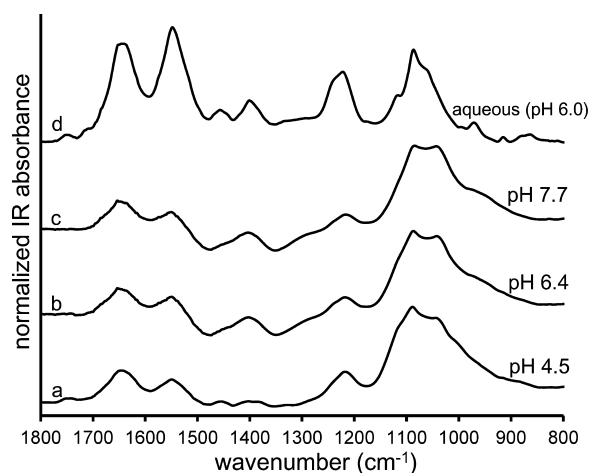


Figure 2. ATR-FTIR spectra collected following 24 h of sorptive interaction between *S. putrefaciens* cells and hematite at the pH values indicated (a–c). Spectrum d is the IR spectrum of an aqueous suspension of *S. putrefaciens* cells (10^9 cells mL^{-1}) at pH 6.0. Negative bands near 1350 and 1480 cm^{-1} in the sorption spectra indicate desorption of carbonate from the hematite surface during cell attachment.

(following 24 h of sorption) at pH 4.5, 6.4, and 7.7 (spectra a–c) to the spectrum of aqueous bacterial cells at pH 6.0 (spectrum d). Notable differences between the spectra of aqueous and hematite-sorbed bacterial cells, and between spectra of sorbed bacterial cells collected at different pH suggest strong interactions between *S. putrefaciens* cells and the hematite surface, modulated by solution pH. Compared to the spectra of aqueous *S. putrefaciens* cells, the spectra of hematite-adhered bacterial cells show a pronounced increase in the intensities of the bands in the $1150\text{--}900\text{ cm}^{-1}$ region relative to those of the other IR vibrations, as well as changes in the band positions and relative intensities of bands within the $1150\text{--}900\text{ cm}^{-1}$ wavenumber range. Notable as well are the negative absorbances observed at ~ 1350 and 1480 cm^{-1} in the spectra

of adhered *S. putrefaciens* cells, which indicate desorption of carbonate groups from the hematite surface during cell attachment, as also observed during (inner-sphere) adsorption of phosphate and borate on iron oxide substrates.^{46,62} The strong negative carbonate absorbances in the pH 6.4 and 7.7 spectra in particular likely reflect the presence of high concentrations of adsorbed carbonate at the hematite surface at these pH values in the absence of competing bacterial surface functionalities.^{53,63}

IR spectra reported by Parikh and Chorover³⁷ for Gram-positive and Gram-negative microbial cells adhered to goethite are similar to the results found here for *S. putrefaciens* cell attachment to hematite. Distinct changes in the $1150\text{--}900\text{ cm}^{-1}$ range in the spectra of adhered cells relative to aqueous cells signaling the importance of bacterial phosphate/phosphonate groups for initiating cell adhesion to the goethite surface³⁷ are noted here for *S. putrefaciens* attachment to hematite as well. These authors assigned the bands at 1087 cm^{-1} to ring vibrations and symmetric P–O stretching bands of PO_2 in phosphate $\nu_s(\text{PO}_2)$, and the band at 1040 cm^{-1} to P–OFe stretching ($\nu(\text{P–OFe})$), and concluded that terminal phosphate/phosphonate and phosphodiester groups are involved in the adhesion of bacterial cells to the goethite surface through formation of inner-sphere complexes.³⁷ The formation of inner-sphere bonds between hematite surface sites and cell wall P-moieties is consistent with the desorption of adsorbed As(V) observed in a previous study during coordination of *S. putrefaciens* cells to the hematite surface,¹⁸ and with the desorption of adsorbed carbonate evident from the IR spectra of adhered cells collected here (Figure 2). The strong IR band intensities of reactive P-groups in the spectra of hematite-sorbed bacterial cells suggest strong interactions leading to enrichment of P-moieties at hematite particle surfaces relative to other bacterial groups. This finding is consistent with the macroscopic results of Omoike and Chorover⁴⁵, who observed preferential removal of P-rich bacterial EPS molecules during sorption on goethite, and is in line with the well documented affinity of orthophosphate for inner-sphere interaction with iron-oxide surfaces.^{46,47,64} Preferential coordination of bacterial P groups through inner-sphere coordination to the hematite surface suggest an important role of these groups in mediating adhesion of *S. putrefaciens* bacterial cells, as previously found for adhesion of cells of *Shewanella oneidensis*, *Pseudomonas aeruginosa*, and *Bacillus subtilis* to the surface of goethite.³⁷

The data presented in Figure 2 also show that the inner-sphere interaction between the bacterial phosphate groups and the hematite surface is pH dependent, as indicated by the differences in the P–O stretching region observed for the spectra of attached bacterial cells collected at different pH values (Figure 2). Lowering the pH from 7.7 to 4.5 leads to the appearance of an additional P–O stretching frequency at $\sim 1125\text{ cm}^{-1}$, while bands at ~ 1050 and 1000 cm^{-1} become less pronounced. This pH dependency is further illustrated in Figure 3, which compares the spectra of adhered microbial cells to those of adsorbed P reference compounds at different pH values in the spectral region containing the P–O ν_3 stretching bands ($1300\text{--}800\text{ cm}^{-1}$). The IR spectra of the surface complexes of the three P reference compounds (spectra c–i) differ substantially from the spectra of their aqueous counterparts (spectra j–m), consistent with inner-sphere coordination of phosphate groups at the hematite surface. The pH dependency of the spectra of adhered *S. putrefaciens* cells

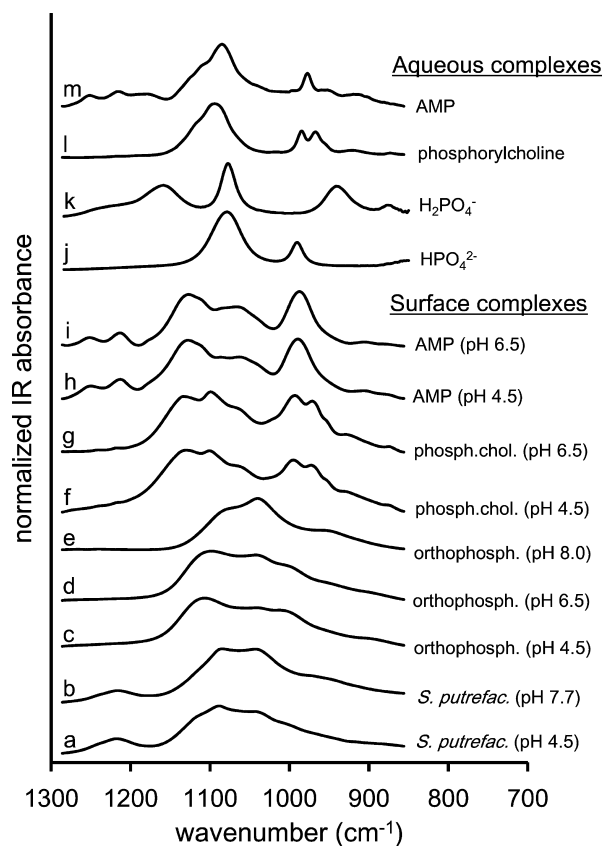


Figure 3. Comparison of the IR frequencies appearing in the spectral region containing the P–O ν_3 stretching bands for the spectra of bacterial phosphate/phosphonate groups attached to the hematite surface (a, b) and adsorbed P reference compounds (c–i). Spectra j–m represent the aqueous species of the reference compounds collected at pH 6.0 (AMP and phosphocholine), pH 4.5 (H_2PO_4^- (aq)) and pH 8.0 (HPO_4^{2-} (aq)).

(spectra a, b) in this frequency region resembles the spectral changes observed as a function of pH for orthophosphate and phosphorylcholine surface complexes on hematite (spectra c–g). For orthophosphate, adsorption at high pH leads to the formation of surface complexes characterized by P–O stretching modes at ~ 1080 , 1050 , and 950 cm^{-1} (Figure 3, spectrum e). Elzinga and Sparks⁴⁶ showed that these complexes are protonated, and suggested that they represent monodentate monoprotonated surface complexes or possibly monodentate surface complexes stabilized by hydrogen bonding to adjacent sites. Lowering pH leads to the appearance of additional orthophosphate surface complexes with bands at ~ 1150 , 1008 , and 980 cm^{-1} (Figure 3, spectra c and d), assigned as monoprotonated bridging bidentate surface complexes,⁴⁶ with the band at 1150 cm^{-1} representing $\nu(\text{P}=\text{O})$, the frequency at 1008 cm^{-1} representing $\nu_{\text{as}}(\text{P}-(\text{OFe})_2)$, and the band at 980 cm^{-1} representing $\nu_{\text{s}}(\text{P}-(\text{OFe})_2)$ or $\nu(\text{P}-\text{OH})$.^{46,47} The speciation of phosphorylcholine surface complexes depends on pH as well, as indicated by the increase in the relative intensity of P–O bands at ~ 1150 and $\sim 1000\text{ cm}^{-1}$ as pH is lowered from 6.5 to 4.5 (spectra f and g), whereas for AMP, no major differences are seen in the IR spectra of surface complexes formed at pH 6.5 versus pH 4.5 (spectra h and i). The changes with pH observed in the P–O stretching bands of bacterial phosphate groups (Figure 3, spectra a and b) indicate that, similar to the surface complexes of the orthophosphate

and phosphocholine reference compounds, the coordination and/or protonation state of bacterial phosphate groups at the hematite surface vary with pH. This implies that the molecular level interactions between bacterial cells and the hematite surface are pH dependent. Assignments of structural changes (surface coordination and/or degree of protonation) associated with the pH dependence observed in the IR data of adhered cells are poorly constrained, as the chemical identity (or identities) of the phosphoryl groups involved is unknown. Band sets with similar P–O stretching frequencies as observed here at 1108 , 992 , and 974 cm^{-1} , and at 1095 , 1011 , and 983 cm^{-1} have been assigned to, respectively, monoprotonated monodentate and nonprotonated bidentate surface complexes of methylphosphonic acid on goethite.⁴⁸ Further studies are needed to assess the specific phosphoryl species involved in the inner-sphere coordination of bacterial cells to the surface of Fe(III)-oxides, and the mechanistic influence of pH on this process.

Macroscopic studies of bacterial adhesion to iron oxide mineral surfaces generally show a decrease in cell attachment as pH increases, which is commonly attributed to electrostatic effects, with build-up of negative iron oxide surface charge with increasing pH making interaction with negatively charged bacterial cells less favorable.^{65–67} The inner-sphere reactions between reactive bacterial groups and hematite surface sites observed here suggest that pH-driven changes in the extent of microbial cell attachment to Fe(III)-oxide surfaces are not solely due to electrostatic effects, but also influenced by competition of hydroxyl groups for inner-sphere coordination at hematite surface sites limiting attachment at higher pH. This is similar to the adsorption of orthophosphate onto Fe(III)-oxides, which involves formation of inner-sphere surface complexes, and decreases with increasing pH.^{46,47,64,68} The pH dependence observed for the mechanisms involved in the inner-sphere interactions between phosphate-based bacterial groups and hematite (Figures 2, 3) suggests that the extent to which cell adhesion induces desorption of adsorbed metalloids (as observed in ref 18–20) may vary with pH as well, since the affinity (and hence competitiveness) of bacterial phosphate groups for the hematite surface likely depend on the attachment mechanisms involved. Further studies are required to correlate pH dependent mechanistic changes in bacterial cell adhesion to the efficiency of cell attachment, and to characterize associated impacts on the mobilization of sorbed metal(loid) impurities.

In addition to varying with pH, spectra obtained during *S. putrefaciens* bacterial cell adhesion also change as a function of time. This is illustrated in Figure 4a, which compares the spectra of adsorbed *S. putrefaciens* cells after sorption for 5 and 24 h at pH 4.5, 6.4, and 7.7. Both the short (5 h) and long-term (24 h) spectra exhibit pronounced phosphate stretching bands, but the frequencies and relative intensities of the ν_3 stretching bands are different for the 5 h versus 24 h spectra collected at each pH value. Moreover, there is a distinct increase in the relative intensities of the bands associated with bacterial functional groups other than P-moieties for the 24 h spectra as compared to the 5 h spectra. This last point is well illustrated by the difference spectra between the various 5 and 24 h sorption spectra (Figure 4a and b), which characterize bacterial adhesion occurring between 5 and 24 h of sorption. The difference spectra show distinct frequencies associated with protein and carboxyl groups in addition to the P–O bands not seen in the short term spectra (Figure 4a, b), demonstrating

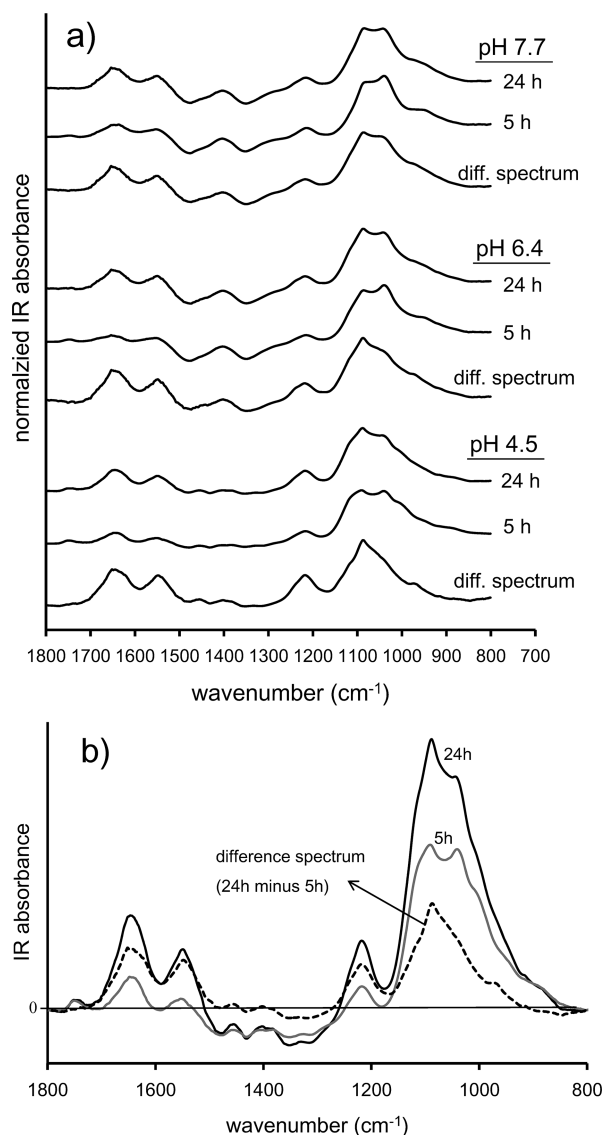


Figure 4. (a) Comparison of the normalized spectra of adhered *S. putrefaciens* cells following 5 and 24 h of sorption at pH 7.7, 6.4, and 4.5, along with the (normalized) difference spectra between the 5 and 24 h sorption spectra characterizing the complexes formed between 5 and 24 h of interaction between *S. putrefaciens* bacterial cells and the hematite surface; (b) non-normalized IR spectra of adhered bacterial cells at pH 4.5 illustrating the relation between the long (24 h) and short-term (5 h) spectra and the difference spectrum calculated from them.

that bacterial adhesion occurring over longer time scales is to a lesser degree associated with preferential attachment of P-based bacterial functional groups in the near-surface region probed by the IR beam than adhesion in the early stages of the attachment process.

Based on the strength of the Fe–O–P bond and absent any indication in the long term IR spectra of detachment of inner-sphere phosphoryl groups from the surface, a likely explanation for the observed time dependency is that the inner-spherically coordinated phosphoryl groups that define cell-hematite interactions at short times may not change or be displaced, but may be supplemented by longer-term attachment of proteinaceous and carboxylated components. Several mechanisms may be involved, including: (i) preferential adsorption of

loosely bound P-rich moieties detaching from bacterial cell walls during the early sorption stages, followed by adhesion of whole cells during later sorption times; (ii) increased proximity of bacterial cells and proteinaceous and carboxylated cell wall components to the hematite surface over longer time scales following initial cell anchoring by P-moieties associated with cell wall EPS macromolecules; and/or (iii) variability in the spatial distribution of cell wall functional groups as observed in a study characterizing *S. putrefaciens* cells using electrostatic force microscopy,³³ where distinct patching of surface charge on *S. putrefaciens* cell walls indicated a heterogeneous distribution of reactive groups over the cell surface, suggesting the possibility of variability in the distribution of functional group types; in this scenario, preferred interaction of high affinity P-rich cell wall areas may occur in the early stages of cell attachment, followed by attachment of lower affinity groups over longer time scales. Further studies are required to assess the time dependence of microbial adhesion processes in more detail. Regardless of cause, however, the time dependent change in chemical composition of the hematite-bacterial cell interface evident from the data presented in Figure 4 suggests that the stability and configuration of bacterial cell adhesion may change over time, which in turn implies that the impact of cell adhesion on sorbed impurities is time dependent as well.

ENVIRONMENTAL IMPLICATIONS

The ATR-FTIR analyses presented here indicate that adhesion of bacterial cells of *S. putrefaciens* to the surface of hematite is associated with preferential inner-sphere coordination of bacterial phosphate/phosphate groups. Both pH and contact time modulate the processes involved in attachment, leading to chemical changes at the mineral surface-cell interface that may influence the significance and impact of cell adhesion on major biogeochemical processes including biofilm formation and microbial transport, microbial reduction of Fe(III) and Mn(III, IV), mineral weathering, and mobilization of sorbed metal(loid) impurities from sorbent surfaces by microbial cell functionalities. The findings from this study are of particular relevance to geochemical environments with substantial microbial populations, such as surface soils and their rhizospheres, where microbe-mineral interactions occur extensively and play a central role in carbon, nutrient, and metal(loid) cycling. The effects of other common surface-reactive compounds (e.g., humic substances and major and trace metal(loid)s) on cell-mineral interactions and microbial attachment in soils require further study.

AUTHOR INFORMATION

Corresponding Author

*Phone: (973) 353 5238; e-mail: elzinga@andromeda.rutgers.edu.

Notes

The authors declare no competing financial interest.

REFERENCES

- (1) Roden, E.; Zachara, J. M. Microbial reduction of crystalline iron(III) oxides: Influence of oxide surface area and potential for cell growth. *Environ. Sci. Technol.* **1996**, *30*, 1618–1628.
- (2) Zhang, M. N.; Ginn, B. R.; Dichristina, T. J.; Stack, A. G. Adhesion of *Shewanella oneidensis* MR-1 to iron (oxy)(hydr)oxides: Microcolony formation and isotherm. *Environ. Sci. Technol.* **2010**, *44*, 1602–1609.

- (3) Rancourt, D. G.; Thibault, P. J.; Mavrocordatos, D.; Lamarche, G. Hydrous ferric oxide precipitation in the presence of non-metabolizing bacteria: Constraints on the mechanism of a biotic effect. *Geochim. Cosmochim. Acta* **2005**, *69*, 553–577.
- (4) Appenzeller, B. M. R.; Duval, Y. B.; Thomas, F.; Block, J. C. Influence of phosphate on bacterial adhesion onto iron oxyhydroxide in drinking water. *Environ. Sci. Technol.* **2002**, *36*, 646–652.
- (5) Donlan, R. M.; Pipes, W. O.; Yohe, T. L. Biofilm formation on cast iron substrata in water distribution systems. *Water Res.* **1994**, *28*, 1497–1503.
- (6) LeChevallier, M. W.; Lowry, C. D.; Lee, R. G.; Gibbon, D. L. Examining the relationship between iron corrosion and the disinfection of biofilm bacteria. *J. Am. Water Works Assoc.* **1993**, *85*, 59–71.
- (7) Marshall, K. C. Adsorption and adhesion processes in microbial growth at interfaces. *Adv. Colloid Interface Sci.* **1986**, *25*, 59–86.
- (8) Kaster, K. M.; Hiorth, A.; Kjeilen-Eilertsen, G.; Boccadoro, K.; Lohne, A.; Berland, H.; Stavland, A.; Brakstad, O. G. Mechanisms involved in microbially enhanced oil recovery. *Transp. Porous Media* **2012**, *91*, 59–79.
- (9) Karimi, M.; Mahmoodi, M.; Niazi, A.; Al-Wahaibi, Y.; Ayatollahi, S. Investigating wettability alteration during MEOR process: A micro/macro scale analysis. *Colloids Surf. B* **2012**, *95*, 129–136.
- (10) Costerton, J. W.; Stewart, P. S.; Greenberg, E. P. Bacterial biofilms: A common cause of persistent infections. *Science* **1999**, *284*, 1318–1322.
- (11) Writer, J. H.; Ryan, J. N.; Barber, L. B. Role of biofilms in sorptive removal of steroidal hormones and 4-nonylphenol compounds from streams. *Environ. Sci. Technol.* **2011**, *45*, 7275–7283.
- (12) Battin, T. J.; Kaplan, L. A.; Newbold, J. D.; Hansen, C. M. E. Contributions of microbial biofilms to ecosystem processes in stream mesocosms. *Nature* **2003**, *426*, 439–442.
- (13) Flemming, H. C. Sorption sites in biofilms. *Water Sci. Technol.* **1995**, *32*, 27–33.
- (14) Arnold, R. G.; DiChristina, T. J.; Hoffmann, M. R. Reductive dissolution of Fe(III) oxides by *Pseudomonas* SP 200. *Biotechnol. Bioeng.* **1988**, *32*, 1081–1096.
- (15) Caccavo, F.; Frolund, B.; Kloeke, F. V.; Nielsen, P. H. Deflocculation of activated sludge by the dissimilatory Fe(III)-reducing bacterium *Shewanella alga* BrY. *Appl. Environ. Microbiol.* **1996**, *62*, 1487–1490.
- (16) Grantham, M. C.; Dove, P. M.; DiChristina, T. J. Microbially catalyzed dissolution of iron and aluminum oxyhydroxide mineral surface coatings. *Geochim. Cosmochim. Acta* **1997**, *61*, 4467–4477.
- (17) Das, A.; Caccavo, F. Dissimilatory Fe(III) oxide reduction by *Shewanella alga* BrY requires adhesion. *Curr. Microbiol.* **2000**, *40*, 344–347.
- (18) Huang, J. H.; Elzinga, E. J.; Brechbuehl, Y.; Voegelin, A.; Kretzschmar, R. Impacts of *Shewanella putrefaciens* strain CN-32 cells and extracellular polymeric substances on the sorption of As(V) and As(III) on Fe(III)-(hydr)oxides. *Environ. Sci. Technol.* **2011**, *45*, 2804–2810.
- (19) Huang, J. H.; Voegelin, A.; Pombo, S. A.; Lazzaro, A.; Zeyer, J.; Kretzschmar, R. Influence of arsenate adsorption to ferrihydrite, goethite, and boehmite on the kinetics of arsenate reduction by *Shewanella putrefaciens* strain CN-32. *Environ. Sci. Technol.* **2011**, *45*, 7701–7709.
- (20) Jones, L. C.; Lafferty, B. J.; Sparks, D. L. Additive and competitive effects of bacterial and Mn oxides on arsenite oxidation kinetics. *Environ. Sci. Technol.* **2012**, *46*, 6548–6555.
- (21) Beveridge, T. J.; Graham, L. L. Surface layers of bacteria. *Microbiol. Mol. Biol. Rev.* **1991**, *55*, 684–705.
- (22) Gadd, G. M. Biosorption: Critical review of scientific rationale, environmental importance and significance for pollution treatment. *J. Chem. Technol. Biotechnol.* **2009**, *84*, 13–28.
- (23) Wingender, J.; Neu, T. R.; Flemming, H.-C. *Microbial Extracellular Polymeric Substances*; Springer-Verlag: Heidelberg, 1999.
- (24) Fein, J. B.; Martin, A. M.; Wightman, P. G. Metal adsorption onto bacterial surfaces: Development of a predictive approach. *Geochim. Cosmochim. Acta* **2001**, *65*, 4267–4273.
- (25) Kelly, S. D.; Kemner, K. M.; Fein, J. B.; Fowle, D. A.; Boyanov, M. I.; Bunker, B. A.; Yee, N. X-ray absorption fine structure determination of pH-dependent U-bacterial cell wall interactions. *Geochim. Cosmochim. Acta* **2002**, *66*, 3855–387.
- (26) Yee, N.; Benning, L. G.; Phoenix, V. R.; Ferris, F. G. Characterization of metal-cyanobacteria sorption reactions: A combined macroscopic and infrared spectroscopic investigation. *Environ. Sci. Technol.* **2004**, *38*, 775–782.
- (27) Burnett, P. G. G.; Daughney, C. J.; Peak, D. Cd Adsorption onto *Anoxybacillus flavithermus*: Surface complexation modeling and spectroscopic investigations. *Geochim. Cosmochim. Acta* **2006**, *70*, 5253–5269.
- (28) Omoike, A.; Chorover, J. Depth profiling adsorption of extracellular polymeric substances (EPS) from *Pseudomonas aeruginosa* (PAO1) onto α -Fe₂O₃ using variable angle ATR-FTIR. *Geochim. Cosmochim. Acta* **2005**, *69*, A676–A676.
- (29) Parikh, S. J.; Chorover, J. ATR-FTIR study of lipopolysaccharides at mineral surfaces. *Colloids Surf. B* **2008**, *62*, 188–198.
- (30) Gao, X. D.; Metge, D. W.; Ray, C.; Harvey, R. W.; Chorover, J. Surface complexation of carboxylate adheres *Cryptosporidium parvum* oocysts to the hematite-water interface. *Environ. Sci. Technol.* **2009**, *43*, 7423–7429.
- (31) Ojeda, J. J.; Romero-Gonzalez, M. E.; Pوران, H. M.; Banwart, S. A. In situ monitoring of the biofilm formation of *Pseudomonas putida* on hematite using flow-cell ATR-FTIR spectroscopy to investigate the formation of inner-sphere bonds between the bacteria and the mineral. *Mineral. Mag.* **2008**, *72*, 101–106.
- (32) Borrok, D.; Turner, B. F.; Fein, J. B. A universal surface complexation framework for modeling proton binding onto bacterial surfaces in geologic settings. *Am. J. Sci.* **2005**, *305*, 826–853.
- (33) Sokolov, L.; Smith, D. S.; Henderson, G. S.; Gorby, Y. A.; Ferris, F. G. Cell surface electrochemical heterogeneity of the Fe(III)-reducing bacteria *Shewanella putrefaciens*. *Environ. Sci. Technol.* **2001**, *35*, 341–347.
- (34) Kosmulski, M. The pH-dependent surface charging and points of zero charge V. Update. *J. Colloid Interface Sci.* **2011**, *353*, 1–15.
- (35) Lower, S. K.; Hochella, M. F.; Beveridge, T. J. Bacterial recognition of mineral surfaces: Nanoscale interactions between *Shewanella* and α -FeOOH. *Science* **2001**, *292*, 1360–1363.
- (36) Xu, L. C.; Logan, B. E. Interaction forces measured using AFM between colloids and surfaces coated with both dextran and protein. *Langmuir* **2006**, *22*, 4720–4727.
- (37) Parikh, S. J.; Chorover, J. ATR-FTIR spectroscopy reveals bond formation during bacterial adhesion to iron oxide. *Langmuir* **2006**, *22*, 8492–8500.
- (38) Li, X.; Logan, B. E. Analysis of bacterial adhesion using a gradient force analysis method and colloid probe atomic force microscopy. *Langmuir* **2004**, *20*, 8817–8822.
- (39) De Kerchove, A. J.; Elimelech, M. Calcium and magnesium cations enhance the adhesion of motile and nonmotile *Pseudomonas aeruginosa* on alginate films. *Langmuir* **2008**, *24*, 3392–3399.
- (40) DiChristina, T. J.; DeLong, E. F. Design and application of rRNA-targeted oligonucleotide probes for the dissimilatory iron- and manganese-reducing bacterium *Shewanella putrefaciens*. *Appl. Environ. Microbiol.* **1993**, *59*, 4152–4160.
- (41) Korenevsky, A.; Beveridge, T. J. The surface Physicochemistry and adhesiveness of *Shewanella* are affected by their surface polysaccharides. *Microbiol.* **2007**, *153*, 1872–1883.
- (42) Jiang, W.; Saxena, A.; Song, B.; Ward, B. B.; Beveridge, T. J.; Myneni, S. C. B. Elucidation of functional groups on Gram-positive and Gram-negative bacterial surfaces using infrared spectroscopy. *Langmuir* **2004**, *20*, 11433–11442.
- (43) Ojeda, J. J.; Romero-Gonzalez, M. E.; Bachmann, R. T.; Edyvean, R. G. J.; Banwart, S. A. Characterization of the cell surface and cell wall chemistry of drinking water bacteria by combining XPS,

FTIR spectroscopy, modeling, and potentiometric titrations. *Langmuir* **2008**, *24*, 4032–4040.

(44) Omoike, A.; Chorover, J.; Kwon, K. D.; Kubicki, J. D. Adhesion of bacterial exopolymers to α -FeOOH: Inner-sphere complexation of phosphodiester Groups. *Langmuir* **2004**, *20*, 11108–11114.

(45) Omoike, A.; Chorover, J. Adsorption to goethite of extracellular polymeric substances from *Bacillus subtilis*. *Geochim. Cosmochim. Acta* **2006**, *70*, 827–838.

(46) Elzinga, E. J.; Sparks, D. L. Phosphate adsorption onto hematite: An *in-situ* ATR-FTIR investigation of the effects of pH and loading level on the mode of phosphate surface complexation. *J. Colloid Interface Sci.* **2007**, *308*, 53–70.

(47) Tejedor-Tejedor, M. I.; Anderson, M. A. Protonation of phosphate on the surface of goethite as studied by CIR-FTIR and electrophoretic mobility. *Langmuir* **1990**, *6*, 602–611.

(48) Barja, B. C.; Tejedor-Tejedor, M. I.; Anderson, M. A. Complexation of methylphosphonic acid with the surface of goethite particles in aqueous solution. *Langmuir* **1999**, *15*, 2316–2312.

(49) Hwang, Y. S.; Lenhart, J. J. Adsorption of C4-dicarboxylic acids at the hematite/water interface. *Langmuir* **2008**, *24*, 13934–13943.

(50) Hwang, Y. S.; Liu, J.; Lenhart, J. J.; Hadad, C. M. Surface complexes of phthalic acid at the hematite/water interface. *J. Colloid Interface Sci.* **2007**, *307*, 124–134.

(51) Kwon, K. D.; Kubicki, J. D. Molecular orbital theory study on surface complex structures of phosphates to iron hydroxides: Calculation of vibrational frequencies and adsorption energies. *Langmuir* **2004**, *20*, 9249–9254.

(52) Sugimoto, T.; Sakata, K.; Muramatsu, A. Formation mechanism of monodisperse pseudocubic α -Fe₂O₃ particles from condensed ferric hydroxide gel. *J. Colloid Interface Sci.* **1993**, *159*, 372–382.

(53) Brechbühl, Y.; Christl, I.; Elzinga, E. J.; Kretzschmar, R. Competitive sorption of carbonate and arsenic to hematite: Combined ATR-FTIR and batch experiments. *J. Colloid Interface Sci.* **2012**, *377*, 313–321.

(54) Hug, S. J. *In Situ* Fourier transform infrared measurements of sulfate adsorption on hematite in aqueous solutions. *J. Colloid Interface Sci.* **1997**, *188*, 415–422.

(55) Roberts, J. A.; Fowle, D. A.; Hughes, B. T.; Kulczykcki, E. Attachment behavior of *Shewanella putrefaciens* onto magnetite under aerobic and anaerobic conditions. *Geomicrobiol. J.* **2006**, *23*, 631–640.

(56) Gaboriaud, F.; Dague, E.; Bailet, S.; Jorand, F.; Duval, J.; Thomas, F. Multiscale dynamics of the cell envelope of *Shewanella putrefaciens* as a response to pH change. *Colloids Surf. B* **2006**, *52*, 108–116.

(57) Gaboriaud, F.; Bailet, S.; Dague, E.; Jorand, F. Probing the modifications of polystyrene surface properties after incubation with the *Shewanella putrefaciens* bacteria at two pH values (4, 10) by atomic force microscopy. *Surf. Interface Anal.* **2007**, *39*, 648–652.

(58) Hug, S. J.; Sulzberger, B. *In situ* Fourier transform infrared spectroscopic evidence for the formation of several different surface complexes of oxalate on TiO₂ in the aqueous phase. *Langmuir* **1994**, *10*, 3587–3597.

(59) Van Bronswijk, W.; Kirwan, L. J.; Fawell, P. D. *In situ* adsorption densities of polyacrylates on hematite nano-particle films as determined by ATR-FTIR spectroscopy. *Vib. Spectrosc.* **2006**, *41*, 176–181.

(60) Rosso, K. M.; Zachara, J. M.; Fredrickson, J. K.; Gorby, Y. A.; Smith, S. C. Nonlocal bacterial electron transfer to hematite surfaces. *Geochim. Cosmochim. Acta* **2003**, *67*, 1081–1087.

(61) Glasauer, S.; Langley, S.; Beveridge, T. J. Sorption of Fe (hydr)oxides to the surface of *Shewanella putrefaciens*: Cell-bound fine-grained minerals are not always formed *de novo*. *Appl. Environ. Microbiol.* **2001**, *67*, 5544–5550.

(62) Peak, D.; Luther, G. W.; Sparks, D. L. ATR-FTIR spectroscopic studies of boric acid adsorption on hydrous ferric oxide. *Geochim. Cosmochim. Acta* **2003**, *67*, 2551–2560.

(63) Van Geen, A.; Robertson, A. P.; Leckie, J. O. Complexation of carbonate species at the goethite surface: Implication for adsorption of

metal ions in natural water. *Geochim. Cosmochim. Acta* **1994**, *58*, 2073–2086.

(64) Arai, Y.; Sparks, D. L. ATR-FTIR spectroscopic investigation on phosphate adsorption mechanisms at the ferrihydrite-water interface. *J. Colloid Interface Sci.* **2001**, *241*, 317–326.

(65) Ams, D. A.; Fein, J. B.; Dong, H. L.; Maurice, P. A. Experimental measurements of the adsorption of *Bacillus subtilis* and *Pseudomonas mendocina* onto Fe-oxyhydroxide-coated and uncoated quartz grains. *Geomicrobiol. J.* **2004**, *21*, 511–519.

(66) Jiang, D.; Huang, Q.; Cai, P.; Rong, X.; Chen, W. Adsorption of *Pseudomonas putida* on clay minerals and iron oxide. *Colloids Surf. B* **2007**, *54*, 217–221.

(67) Kim, S. B.; Park, S. J.; Lee, C. G.; Choi, N. C.; Kim, D. J. Bacteria transport through goethite-coated sand: Effects of solution pH and coated sand content. *Colloids Surf. B* **2008**, *63*, 236–242.

(68) Persson, P.; Nilsson, N.; Sjöberg, S. Structure and bonding of orthophosphate ions at the iron oxide-aqueous interface. *J. Colloid Interface Sci.* **1996**, *177*, 263–275.